Energy & Environmental Science

RSC Publishing

PAPER

View Article Online
View Journal | View Issue

Cite this: *Energy Environ. Sci.*, 2013, **6**, 2682

Hydrogen production through oxygenic photosynthesis using the cyanobacterium *Synechocystis* sp. PCC 6803 in a bio-photoelectrolysis cell (BPE) system†

Alistair J. McCormick,[a] Paolo Bombelli,[a] David J. Lea-Smith,[a] Robert W. Bradley,[a] Amanda M. Scott,[b] Adrian C. Fisher,[b] Alison G. Smith[c] and Christopher J. Howe*[a]

Microbial electrolysis cells (MECs) represent an emerging technology that uses heterotrophic microbes to convert organic substrates into fuel products, such as hydrogen gas (H_2). The recent development of biophotovoltaic cells (BPVs), which use autotrophic microbes to produce electricity with only light as a substrate, raises the possibility of exploiting similar systems to harness photosynthesis to drive the production of H_2. In the current study we explore the capacity of the cyanobacterium *Synechocystis* sp. PCC 6803 to generate electrons by oxygenic photosynthesis and facilitate H_2 production in a two-chamber bio-photoelectrolysis cell (BPE) system using the electron mediator potassium ferricyanide ($[Fe(CN)_6]^{3-}$). The performance of a wild-type and mutant strain lacking all three respiratory terminal oxidase activities (*rto*) was compared under low or high salt conditions. The *rto* mutant showed a decrease in maximum photosynthetic rates under low salt (60% lower P_{max} than wild-type) but significantly increased rates under high salt, comparable to wild-type levels. Remarkably, *rto* demonstrated a 3-fold increase in $(Fe[CN]_6)^{3-}$ reduction rates in the light under both low and high salt compared to the wild-type. Yields of H_2 and efficiency parameters were similar between wild-type and *rto*, and highest under high salt conditions, resulting in a maximum rate of H_2 production of 2.23 $\pm$ 0.22 ml H_2 l^{-1} h^{-1} (0.68 $\pm$ 0.11 mmol H_2 [mol Chl]$^{-1}$ s^{-1}). H_2 production rates were dependent on the application of a bias-potential, but all voltages used were significantly less than that required for water electrolysis. These results clearly show that production of H_2 using cyanobacteria is feasible without the need to inhibit photosynthetic O_2 evolution. Optimising the balance between the rates of microbial-facilitated mediator reduction with H_2 production may lead to long-term sustainable H_2 yields.

Received 11th February 2013
Accepted 3rd July 2013

DOI: 10.1039/c3ee40491a

www.rsc.org/ees

Broader context box

Bioelectrochemical systems have emerged as a promising technology for energy recovery and the production of valuable fuel products such as H_2 gas. In microbial electrolysis cells (MECs), heterotrophic bacteria consume organic compounds to drive the electrochemical production of H_2. Here we report a two-chamber bio-photoelectrolysis cell (BPE) system for producing H_2 that uses light as a substrate. In the anodic compartment of the BPE the cyanobacterium *Synechocystis* sp. PCC 6803 was used to generate electrons by oxygenic photosynthesis, with H_2 produced in the cathodic compartment. In addition, we studied the effects of mutations abolishing the terminal oxidases of the respiratory electron transport chain, with the striking result that a mutant (*rto*) showed three-fold higher rates of reduction of the electron mediator ferricyanide than the wild-type strain. This is one of the first examples of O_2-evolving autotrophs being used to facilitate sustainable H_2 production without the need to inhibit photosynthetic O_2 evolution or establish anaerobic conditions in the culture medium. Further increases in output might be achieved using suitable mutants.

Introduction

Hydrogen gas (H_2) has many merits as a clean energy resource. Although there are several chemical processes by which H_2 can be produced,[1] microbial biotechnologies are particularly attractive as they are renewable and often relatively cheap to maintain. Under anaerobic conditions, heterotrophic microbes can produce H_2 through fermentation of carbohydrate-rich suspensions, including industrial and municipal waste water.[2,3] Alternatively, photosynthetic microbes are able to facilitate photobiological H_2 production (biophotolysis).[2–6]

[a]*Department of Biochemistry, University of Cambridge, Hopkins Building, Downing Site, CB2 1QW, UK. E-mail: ch26@cam.ac.uk; Fax: +44 (0)1223 333 345; Tel: +44 (0)1223 333 688*

[b]*Department of Chemical Engineering and Biotechnology, University of Cambridge, New Museums Site, Pembroke Street, CB2 3RA, UK*

[c]*Department of Plant Sciences, University of Cambridge, Downing Site, CB2 3EA, UK*

† Electronic supplementary information (ESI) available. See DOI: 10.1039/c3ee40491a

Using microbes capable of oxygenic photosynthesis, H_2 can be produced using abundant and sustainable natural resources, such as sunlight and water, without the requirement for organic supplements. However, in reports to date with green microalgae or cyanobacteria, substantial restrictions have been imposed on the bioreactor operating conditions in order to generate significant quantities of H_2. For example, H_2 production with green algae can occur only under near anaerobic conditions, as the primary catalytic enzyme involved (Fe–Fe hydrogenase) is inhibited by oxygen (O_2). Thus far, sustained H_2 production with algae (*e.g. Chlamydomonas* sp.) has been achieved only in the presence of a major decrease in activity of photosystem II – the O_2-evolving complex of the photosynthetic apparatus. This was achieved using sulphur deprivation to decrease the O_2 production rate below the rate of O_2 use through mitochondrial respiration.[5,7,8] To produce H_2 with filamentous cyanobacteria, such as *Anabaena* sp., nitrogen sources in the culture media must be depleted to allow H_2-producing heterocysts to form.[4] Unicellular cyanobacteria require the removal of O_2 from the growth medium for sustained H_2 production.[4,9] Extensive work in this field has been carried out to identify phenotypes/mutants with increased O_2 tolerance and H_2 yields.[6,9–13]

Microbes can also be utilised in bioelectrochemical systems (BESs) to generate an electromotive force, which can then be used for power production (in the form of electricity) or the generation of secondary products at the cathode. Much attention recently has been given to the development of novel BESs for producing a variety of useful secondary products, including H_2.[3,14] In particular, progress has been made in the field of microbial electrolysis cells (MECs), which typically use heterotrophic bacteria attached to an anodic electrode to catalyse the cathodic production of H_2 in a single- or two-chamber system.[15–17] The production of H_2 in MECs is facilitated by the heterotrophic bacteria and thermodynamically unfavourable. Hence such systems do require additional energy inputs in the form of organic substrate and an applied bias-potential (typically provided by a power supply unit or a potentiostat) to drive the reaction forward.[14]

BESs that generate electricity in a light-dependent manner using cyanobacteria and algae (known as biological photovoltaic cells [BPVs]) have also received increased attention recently.[18–23] However, to date no studies have reported the use of oxygenic photosynthetic microbes at the anode for the cathodic production of H_2 in a MEC-type system. In MECs the cathode requires a strictly anaerobic environment, as the formation of water from O_2 and protons is energetically more favourable than the production of H_2 from protons alone.[14] The process of H_2 production is currently considered unfeasible in the presence of autotrophic microbes that produce O_2 during the photosynthetic process. Nevertheless, it may be possible to facilitate sustainable H_2 production using autotrophic microbes if the chambers are separated, for example, by an anionic or cationic exchange membrane.[21] A ruthenium-based "artificial photosynthesis" photochemical cell was recently described that achieved simultaneous production of O_2 (and H^+) and H_2 by separating the O_2-producing anodic and H_2-producing cathodic chambers by a proton permeable membrane.[24] Bora *et al.*[25] recently highlighted the value of constructing bio-photoelectrochemical cells using biomolecule-modified electrodes separated by a Nafion® membrane. For both artificial and biological systems the challenge then lies in optimising the efficiency of H_2 production, such that external energy inputs (*e.g.* applied bias-potentials) do not outweigh potential energy gains from the H_2 recovered.[14,26] At a minimum, the microbial electrolysis process should require substantially less energy investment than that required for water electrolysis.[14]

Several microbial species, including green algae, diatoms and cyanobacteria, are readily able to photo-catalyse the reduction of soluble extracellular electron mediators, such as potassium ferricyanide ($[Fe(CN)_6]^{3-}$) to potassium ferrocyanide ($[Fe(CN)_6]^{4-}$).[27–30] The electrons harvested by $(Fe[CN]_6)^{4-}$ can then be used as a recyclable fuel source at the anode for electricity production (such as in BPV devices[21]), or production of secondary products at the cathode in what can be referred to as a bio-photoelectrolysis cell (BPE). The model cyanobacterial strain *Synechocystis* sp. PCC 6803 is an ideal candidate species to investigate BPEs for several reasons: (i) its genome is fully sequenced and the strain is readily transformable[31,32] (ii), it is euryhaline[33] and (iii) it readily reduces $(Fe[CN]_6)^{3-}$ and there is no obvious toxicity from $(Fe[CN]_6)^{4-/3-}$ ions at relatively high concentrations (up to 20 mM).[21] Recent work has demonstrated that growth rates of *Synechocystis* are unaffected by the presence of $(Fe[CN]_6)^{4-/3-}$, and cultures show variable $(Fe[CN]_6)^{3-}$ reduction rates depending on environmental conditions and media salinity.[30] Furthermore, a *Synechocystis* mutant, referred to here as *rto*, lacking all three terminal oxidases (cyd, cox [ctaI], ARTO [ctaII]) of the respiratory electron transport chain[34] has been demonstrated to increase H_2 production in a culture at low O_2 concentration.[9] Since terminal oxidases act as alternative electron sinks, we hypothesised that the absence of those terminal oxidases would be likely to lead to a more reduced intracellular environment in the *rto* mutant, which may then favour the reduction of alternative electron acceptors. Whether specific extracellular or intracellular conditions would substantially affect the rate of exoelectrogenic activity is not well explored,[35,36] but may be of great interest to several BES technologies.

We therefore set out to test if a two-chamber BPE system could be used to facilitate H_2 production with *Synechocystis* strains and $(Fe[CN]_6)^{3-}$ as an electron mediator in either low or high salt grown cultures. Although a bias-potential was required to drive the production of H_2 (1.0–1.4 V), all applied bias-potentials were lower than that required for water electrolysis (*ca.* 2.2 V).[37] This is, to our knowledge, the first time that unicellular O_2-evolving autotrophs have been used to facilitate sustained H_2 production for several hours without the need to inhibit photosynthetic O_2 evolution or establish anaerobic conditions in the culture medium. Furthermore, this is the first report of an MEC-type system that has successfully harnessed the exoelectrogenic activities of O_2-evolving autotrophs by spatially and temporally separating O_2 and H_2 evolving processes in a single system.

Results

Photosynthesis and respiration

In the BPE system used here (Fig. 1), photosynthesis and respiration can be considered as the primary sources of electrons for H_2 production. In typical growth medium (*i.e.* low salt), the maximum photosynthetic O_2 evolution rate (P_{max}) of the *rto* mutant was 60% lower than wild-type *Synechocystis* cultures (Fig. 2; Table 1). The absence of the three respiratory electron transport chain terminal oxidases in *rto* resulted in significantly decreased respiration rates (average 57% lower than wild-type under both high and low salt) (ESI Fig. 1†).

Growth in high salt medium did not appear to affect photosynthesis or respiration in wild-type cultures (Fig. 2, Table 1). However, photosynthetic rates were significantly higher than in low salt medium for *rto*, including a remarkable 85% and 96% increase in P_{max} and apparent quantum efficiency (AQE), respectively. Under high salt conditions, P_{max} and AQE of *rto* were partially restored to levels similar to wild-type cultures (Fig. 2). For all cultures tested, saturating light levels were reached at approximately 200 μE m^{-2} s^{-1}. This intensity was used for all further experiments with the BPE system in the light.

Potassium ferricyanide reduction and regeneration

In the current system the operation of the BPE device was separated into two stages: the "fuelling phase" and "H_2 production phase" (Fig. 1C). The reduction of $(Fe[CN]_6)^{3-}$ during the fuelling phase is closely linked to the theoretically achievable H_2 yields. Therefore identifying strains and environmental conditions that facilitate increased $(Fe[CN]_6)^{3-}$ reduction rates is of great importance. Consequently, we measured $(Fe[CN]_6)^{3-}$ reduction rates under different conditions for the wild-type and *rto* strains. Each cell culture was initially subjected to dark or light conditions for *ca.* 12 h following inoculation in the device with $(Fe[CN]_6)^{3-}$ (Fig. 3). As expected, $(Fe[CN]_6)^{3-}$ reduction rates were lower in the dark compared to the light, indicating that photosynthetic reactions facilitate increased reduction rates. Furthermore, $(Fe[CN]_6)^{3-}$ reduction rates were typically higher in high salt compared to low salt conditions for both wild-type and *rto* cultures.

For cultures at low salt concentrations, *rto* showed slightly higher reduction rates under light and dark conditions compared to the wild-type. However, at high salt concentrations *rto* showed a striking 6-fold and 3-fold increase in the specific rate of $(Fe[CN]_6)^{3-}$ reduction compared to the wild-type in high salt grown under dark and light, respectively (Fig. 3). This resulted in significantly greater $(Fe[CN]_6)^{3-}$ reduction efficiencies ($FeCN^-_{QE}$) for *rto* under both low and high salt conditions (Table 1). In all cases, culture densities were measured regularly and did not show any significant differences before and after measurements.

When the circuit was closed during the H_2 production phase (Fig. 1C), $(Fe[CN]_6)^{4-}$ (redox potential of 420 mV at pH 7) was oxidised at a constant rate (Fig. 4A) dependent on the bias-potential applied (discussed below). Oxidation rates during operation were typically greater than reduction rates

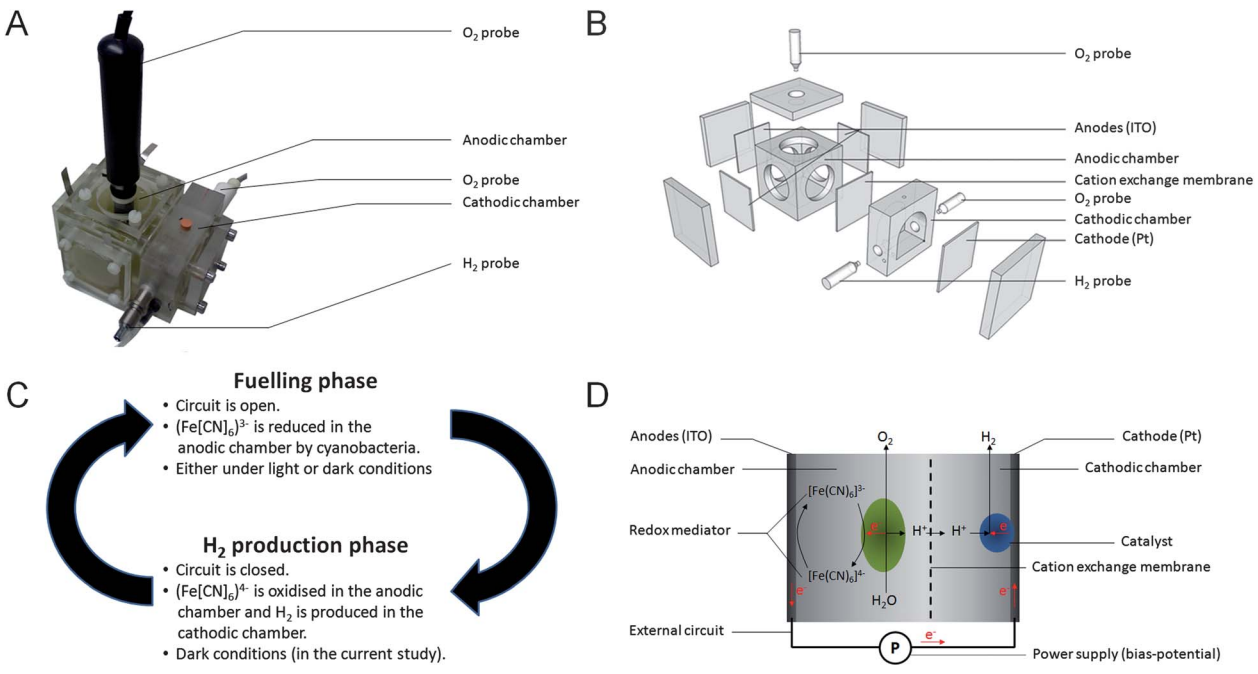

Fig. 1 Construction of a two-chamber bio-photoelectrolysis (BPE) device. An indium tin oxide (ITO) anode was connected to a Pt-coated titanium cathode *via* an external circuit in a two-chamber design separated by a cation exchange membrane (CEM) (A and B). Cyanobacterial cultures were maintained in the anodic chamber, producing O_2 in the light and reducing a redox mediator $[Fe(CN)_6]^{3-}$ to $[Fe(CN)_6]^{4-}$ in the "fuelling phase" (C). Following reduction, $[Fe(CN)_6]^{4-}$ was used as a recyclable electron supply at the anode in the "H_2 production phase". Facilitated by a bias-potential provided from an external power supply (D), current harvested from the anode and protons diffusing through the CEM separating the chambers were used to drive H_2 production at the cathode. H_2- and O_2-sensing electrodes monitored the gas production, whilst a multimeter measured the current and voltage in the external circuit.

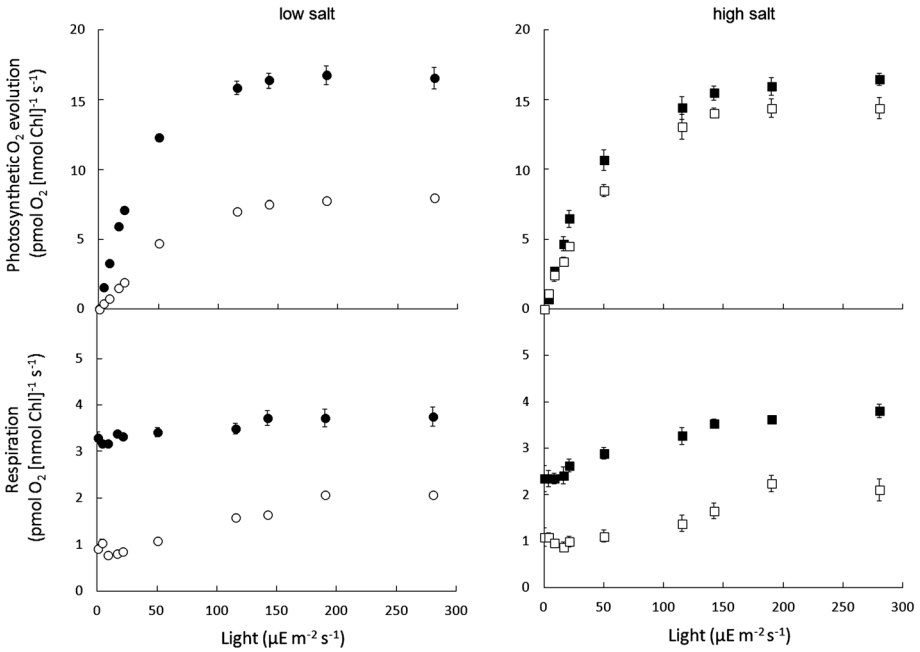

Fig. 2 Photosynthetic light response curves and respiration rates of *Synechocystis* sp. PCC 6803 wild-type and *rto* mutant strains. Cultures ($N = 4$) were pre-grown and tested under high or low salt conditions and measured in the presence of $[Fe(CN)_6]^{3-}$ (1 mM). Respiration rates were measured in the dark period following each light measurement. The maximum photosynthetic O_2 evolution rate (P_{max}) and apparent PSII quantum efficiency (AQE) for wild-type (black circles, squares) and *rto* (white circles, squares) are indicated in Table 1.

Table 1 Photosynthetic performances and substrate turnover efficiencies of cultures used to drive H_2 production. The maximum photosynthetic O_2 evolution rate (P_{max}), dark respiration rate (R_d), maximum respiration rate in the light (R_{max}), apparent PSII quantum efficiency (AQE), actual quantum efficiency at P_{max} (QE_{max}) and the efficiency of $[Fe(CN)_6]^{3-}$ reduction at P_{max} ($FeCN^-_{QE}$) were derived from measurements in Fig. 2 and 4B. The values are the mean ± SE ($N = 4$) and are followed by letters indicating significant difference as in Fig. 3

	Wild-type		*Rto*	
	Low salt	High salt	Low salt	High salt
P_{max} (pmol O_2 [nmol Chl]$^{-1}$ s^{-1})	18.7 ± 1.8 a	20.1 ± 1.4 a	7.5 ± 0.3 c	13.8 ± 0.9 b
R_d (pmol O_2 [nmol Chl]$^{-1}$ s^{-1})	3.5 ± 0.7 a	2.4 ± 0.7 a	0.7 ± 0.1 b	1.3 ± 0.4 b
R_{max} (pmol O_2 [nmol Chl]$^{-1}$ s^{-1})	3.7 ± 0.2 a	3.8 ± 0.2 a	1.6 ± 0.1 b	1.6 ± 0.4 b
AQE (%)	32 ± 2 a	31.1 ± 5.5 a	8.1 ± 0.5 c	15.9 ± 2.2 b
QE_{max} (%)	8.8 ± 0.9 a	9.5 ± 0.6 a	3.5 ± 0.2 c	6.5 ± 0.4 b
$FeCN^-_{QE}$ (%)	2.9 ± 0.3 a	7.1 ± 0.5 b	19 ± 0.9 c	26.8 ± 1.8 d

under open circuit conditions (Fig. 4B), indicating that the rate of $(Fe[CN]_6)^{4-}$ production was not high enough to facilitate a continual substrate supply for H_2 production. Following complete re-oxidation, the device was disconnected and the cultures were given time to re-reduce $(Fe[CN]_6)^{3-}$ either in dark or light conditions. No significant differences in culture reduction rates were observed between successive reduction cycles.

H_2 production rates and efficiencies

The production of H_2 in the cathodic chamber of the BPE system required an applied bias-potential and $(Fe[CN]_6)^{4-}$ as the anodic substrate (ESI Fig. 2†). No H_2 was produced when $(Fe[CN]_6)^{4-/3-}$ was not present in the anodic chamber with *Synechocystis* cells, regardless of the bias-potentials typically applied (1.0–1.4 V) (Fig. 5). Under those conditions, appreciable H_2 production was only seen when 4.0 V of bias-potential was applied. At such high voltages this observation was likely to be attributable to water electrolysis in the cathodic chamber. In the absence of added $(Fe[CN]_6)^4$, the only source for H_2 production between 1.0 and 1.4 V is therefore that generated by biological reduction of $(Fe[CN]_6)^{3-}$.

Following reduction of $(Fe[CN]_6)^{3-}$ to $(Fe[CN]_6)^{4-}$ in the presence of cells in the anodic chamber, the device was connected and a bias-potential applied. During these experiments, all H_2 production proceeded under dark conditions. The rate of H_2 production increased with increasing bias-potential (Fig. 5). Rates were typically higher under high compared to low salt conditions, with a maximum rate of 2.23 ± 0.22 ml H_2 l^{-1} h^{-1} (specific rate of 0.68 ± 0.11 mmol H_2 [mol Chl]$^{-1}$ s^{-1}) in high salt achieved at an applied bias-potential of 1.4 V (Fig. 5). Based

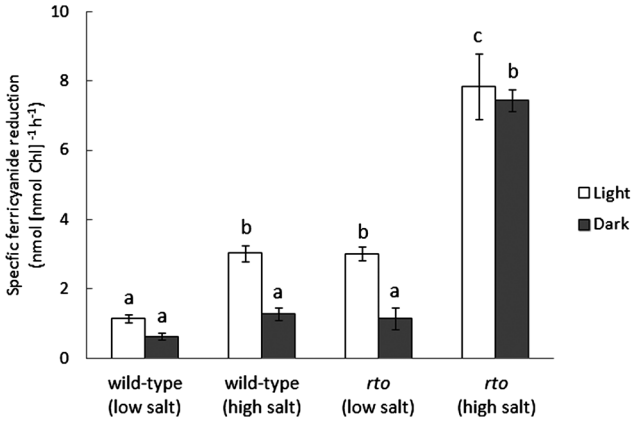

Fig. 3 Specific rates of $[Fe(CN)_6]^{3-}$ reduction by *Synechocystis* sp. PCC 6803 within the device. Cultures were grown and tested in either low or high salt media. Reduction rates of $[Fe(CN)_6]^{3-}$ were measured in the light (200 μE m^{-2} s^{-1}) or dark for approximately 12 h. For experiments conducted in the light (or in the dark), letters above the mean ± SE (standard error) bars ($N = 4$) indicate a difference in reduction rate; where a, b and c indicate significant difference between cultures ($P < 0.05$). Thus, the result labelled 'a' obtained in the light is significantly different from those labelled 'b' or 'c', but those labelled 'b' are not significantly different from one another although they are significantly different from that labelled 'c'. The results labelled 'a' in the dark are not significantly different from one another, but are significantly different from that labelled 'b'. All reduction rates reported were normalised against the natural $[Fe(CN)_6]^{3-}$ reduction rates in the absence of cells.

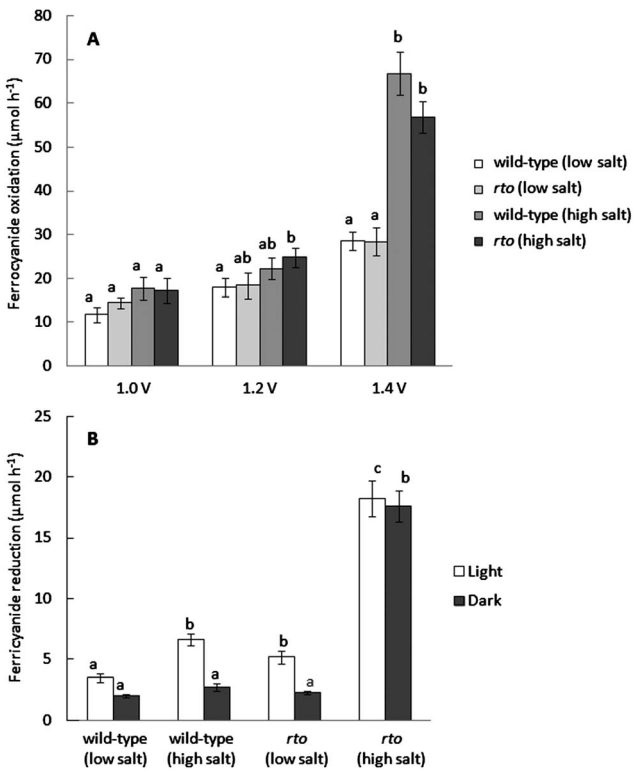

Fig. 4 Turnover rates of $[Fe(CN)_6]^{4-/3-}$ inside the device. $[Fe(CN)_6]^{4-}$ oxidation rates ($N = 4$) under different applied bias-potentials (A) and $[Fe(CN)_6]^{3-}$ reduction rates in the light and dark (adapted from Fig. 3 for comparison) (B) are shown for wild-type and *rto* mutant strains cultured in high or low salt media. (A) letters above the mean ± SE bars indicate significant differences between cultures at each applied potential ($P < 0.05$); (B) letters indicate significant differences among measurements in the light or among measurements in the dark, as in Fig. 3.

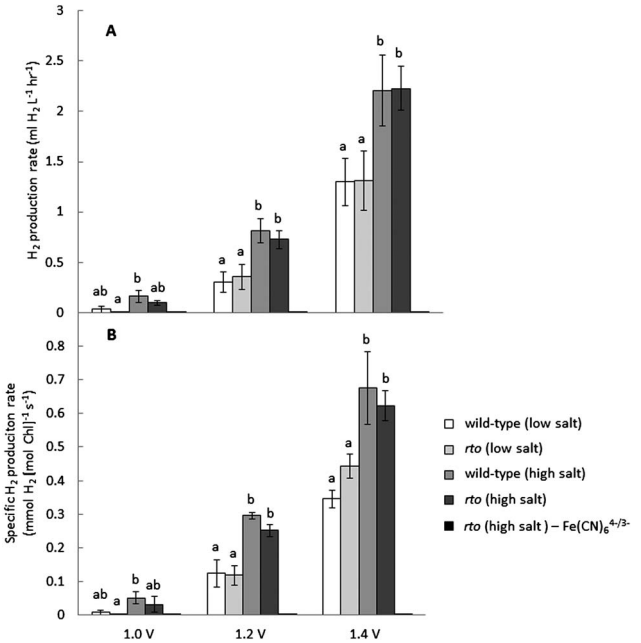

Fig. 5 H_2 production rates of the BPE device at different applied bias-potentials. Both actual (A) and specific (B) H_2 production rates are indicated for each culture. Letters above the mean ± SE bars ($N = 4$) indicate significant differences among measurements at individual bias potentials. A control treatment (the *rto* mutant in high salt medium without $[Fe(CN)_6]^{4-/3-}$) is included.

on the complete reduction of $(Fe[CN]_6)^{3-}$ to $(Fe[CN]_6)^{4-}$ (1 mM) in the anodic chamber prior to connecting the device, this rate could be maintained for *ca.* 4 hours before $(Fe[CN]_6)^{4-}$ levels were depleted. There were no significant differences in H_2 production rates between wild-type or *rto* cultures, indicating that increased H_2 production rate was a result of higher salinity rather than culture type. It is likely that increased H_2 production rates in high salt were attributable to increased solution conductivity (ESI Table 1†).

The ratio of $(Fe[CN]_6)^{4-}$ usage to current production (coulombic efficiency [C_E]), was between 95 and 100% under all applied bias-potentials tested (Table 2), indicating a high

Table 2 Characteristics of the BPE device with different cultures and applied bias-potentials. The ratio of charge to substrate usage (coulombic efficiency, C_E), cathodic H_2 recovery (r_{cat}) and overall H_2 recovery (r_{H_2}) are shown at three different applied bias-potentials (1.0–1.4 V) for each culture ($N = 4$). Calculations were adapted from Logan *et al.*[14] as defined in the Experimental section

	Wild-type		*Rto*	
	Low salt	High salt	Low salt	High salt
C_E (%) – 1 V	98.3 ± 2	96.5 ± 3	95.3 ± 4	99.5 ± 1
C_E (%) – 1.2 V	97.8 ± 2	99.4 ± 1	97.2 ± 3	98.6 ± 2
C_E (%) – 1.4 V	97 ± 2	97.2 ± 2	96 ± 1	97.7 ± 2
r_{cat} (%) – 1 V	4.3 ± 1	4.4 ± 2	4.3 ± 0.4	4.3 ± 2
r_{cat} (%) – 1.2 V	14.4 ± 1	17.2 ± 3	13.9 ± 1	11.7 ± 2
r_{cat} (%) – 1.4 V	20 ± 3	20.5 ± 2	18.5 ± 3	20.1 ± 2
r_{H_2} (%) – 1 V	4.1 ± 1	4.2 ± 2	4.1 ± 0.4	4.2 ± 1
r_{H_2} (%) – 1.2 V	14.1 ± 0.4	17.1 ± 3	13.4 ± 1	11.5 ± 2
r_{H_2} (%) – 1.4 V	19.4 ± 2	20 ± 2	17.8 ± 3	19.7 ± 1

conversion efficiency of $(Fe[CN]_6)^{4-}$ into usable charge at the anode. Overall hydrogen recovery (r_{H_2}) increased with increasing applied bias-potentials, reaching a maximum r_{H_2} at 1.4 V of *ca.* 20%. It is likely that at lower voltages, slower reaction rates and system inefficiencies allow for competition of electrons at the cathode from more thermodynamically favourable acceptors (*e.g.* small amounts of O_2 leakage) and decrease possible H_2 yields.[17] No differences in efficiencies were observed for BPEs without cells in the anode (ESI Fig. 2†), indicating that the presence of cells did not influence the H_2 production phase.

Discussion

This is, to our knowledge, the first example where oxygenic photosynthesis in cyanobacteria has been harnessed in an MEC-type system to produce a source of reducing equivalents for the production of H_2. In the present study the production of H_2 takes place without the need to inhibit the O_2-evolving photosystem II complex. Separation of "O_2 evolution" and "H_2 production" was achieved using a two-chamber BPE system that provided a spatial and temporal partitioning of photosynthetic O_2 evolution in the anodic chamber and subsequent H_2 synthesis in the cathodic chamber (Fig. 1). Charge was initially captured from *Synechocystis* cells using a recyclable extracellular electron mediator ($[Fe(CN)_6]^{4-/3-}$) that, with the addition of an applied bias-potential, could then be utilised as a substrate for H_2 production. Although previous work has described similar systems for electricity production[18,19,21,38] the results of the current study suggest that the production of secondary products and even desalination as demonstrated with BES systems employing heterotrophic microbes[39–41] may also be feasible with photosynthetic microbes.

The two-stage cycle method outlined in this paper (Fig. 1C) relied on an initial substrate accrual period (the fuelling phase) to facilitate the complete reduction of $(Fe[CN]_6)^{3-}$ to $(Fe[CN]_6)^{4-}$ in the anodic chamber, followed by a H_2 production phase (Fig. 5). Although it is likely that $(Fe[CN]_6)^{3-}$ is still reduced in the anodic chamber during the production of H_2, the time taken for complete oxidation of $(Fe[CN]_6)^{4-}$ depended on the bias-potential applied, with a maximum rate of 2.23 ± 0.22 ml H_2 l^{-1} h^{-1} (specific rate of 0.68 ± 0.11 mmol H_2 [mol Chl]$^{-1}$ s^{-1}) for *ca.* 4 hours. The resulting yields compared favourably with existing photobiological H_2 production studies. The specific H_2 production rates achieved here are comparable but more sustained than a recent study with transgenic *Chlamydomonas reinhardtii*.[12] Using an inducible chloroplast gene expression system, Surzycki *et al.*[12] showed that the activity of photosystem II could be transiently inhibited, resulting in a specific H_2 production rate of 1 mmol H_2 [mol Chl]$^{-1}$ s^{-1} that was sustained for a maximum of 1.5 hours. The overall rates we observed were also similar to those reported in other published photobiological H_2 production studies using sulphur-deprived *Chlamydomonas*, which range from 0.58 to 2.35 ml H_2 l^{-1} h^{-1}.[7,8] It is difficult to compare our specific rates directly with those studies, as reactor cultures that undergo cycles of sulphur deprivation typically show large variations in chlorophyll content depending on the particular point of the cycle.[7,8,42]

The energy inputs required for achieving similar rates of H_2 production are substantially smaller for BPEs in comparison with water electrolysis and photobiological techniques. BPE systems primarily need an energy input in the form of a bias-potential. This energy input is required to overcome the potential gap between the anodic reaction (oxidation of electron mediator) and the cathodic reaction (production of H_2) (ESI Fig. 3†). Using $(Fe[CN]_6)^{4-/3-}$ as the electron mediator, this gap cannot be smaller than 0.84 V (at standard atmospheric pressure and pH 7). To allow for additional internal systemic constraints (*e.g.* electrode over-potentials),[14] the bias-potentials used in the current study were between 1.0 and 1.4 V. These values are 55–36% smaller than the potential required to generate H_2 *via* water electrolysis (*ca.* 2.2 V).[37]

The performance of the BPE system used in the current study still compares unfavourably to the typical H_2 recoveries and efficiencies attained in MEC systems.[15–17] Typical r_{H_2} for MECs range from 70–95%, depending on reactor design and organic substrate used, which are achieved at significantly lower bias-potentials (0.2–1.0 V) than used here (Table 2). Nevertheless, BPE systems do appear comparable in terms of C_E, with values of greater than 95% for all applied potentials tested. One of the principal advantages of BPEs such as that described here is that the microbes, and consequently the system, are driven by light. No organic substrate is required. This decreases the inherent complexity of the system compared to MFCs/MECs, where feed stocks must be carefully monitored, as differences in substrate can cause large fluctuations in performance.[17] Moreover, the requirement for feed stocks will incur several additional costs. For example, waste water feed stocks must typically be demineralised to avoid deposits on the electrodes and corrosion.[2]

One of our main aims was to compare the performance of wild-type cultures to the mutant strain *rto*. Photosynthetic O_2 evolution of *rto* returned to near wild-type levels when grown in high salt (Fig. 2). The mutant also showed increased $(Fe[CN]_6)^{3-}$ reduction rates compared to the wild-type under high salt (Fig. 3), suggesting that cyanobacteria can be genetically and environmentally optimised to increase extracellular electron transfer rates and thus energy yields in BPE-type systems. The reason(s) for the remarkable increase in photosynthesis and $(Fe[CN]_6)^{3-}$ reduction rates in *rto* mutants under high salt conditions remains to be fully investigated. Increased media salinities typically result in an increase in conductivity, which can lead to a rise in cellular exoelectrogenic activity.[14] High salt conditions may also have facilitated an alternative respiratory route in the *rto* mutant (*i.e.* an alternative electron sink), resulting in the increase in $FeCN^-_{QE}$ observed (Table 1). It is not yet clear whether the observed increase in photosynthetic activity for *rto* (as indicated by O_2 evolution) was the direct cause of the increase in cellular exoelectrogenic activity as high salt also led to increased rates of $(Fe[CN]_6)^{3-}$ reduction in the dark. Salt stress response is well studied in *Synechocystis* and leads to a multitude of changes in both intracellular and plasma membrane protein levels.[43,44] Drawing on that work, a comparison of the changes in plasma membrane protein abundance between wild-type and *rto* in response to high salt may lead to a clearer understanding of proteins involved in extracellular electron transfer.

Our results indicate that there is substantial scope for optimising the balance between mediator turnover rates with H_2 production, which may lead to long-term sustainable H_2 yields using BPE systems. In terms of optimising the current setup, increases in *Synechocystis* cell concentrations, $(Fe[CN]_6)^{3-}$ and light have previously been shown to improve performance in BPV systems (Bombelli *et al.*, 2011). Recent evidence does suggest that other cyanobacterial species, such as *Synechococcus* sp. WH 5701, may have a higher capacity for extracellular electron transport compared to *Synechocystis*.[22,30] It is possible that alternative electron mediator compounds with a lower electrode potential could further reduce the bias-potential required, thus improving energy efficiencies and potential H_2 yields.[45] For example, 2,6-dichlorophenol-indophenol (DCPIP) has a potential of 290 mV at pH 7, which is 130 mV less than $(Fe[CN]_6)^{4-/3-}$.[46] Even in the current study, the highest $(Fe[CN]_6)^{3-}$ reduction rates seen for *rto* in high salt (Fig. 4B) were similar to the average $(Fe[CN]_6)^{4-}$ oxidation rate observed at applied potentials of 1.0 V or 1.2 V (Fig. 4A). Future work will focus on screening different species and mutants under varying growth conditions, exploring the potential of alternative redox mediators and improvements in reactor design. The latter should include further characterisation of the multitude of electrochemical-related bottlenecks that may affect performance as seen in other BES systems, such as electrode material, spacing, orientation and the area and type of exchange membrane used.[14,47,48]

Conclusions

The current work advances on previous photobiological H_2 production methods by providing a novel and robust BES-based solution that overcomes many of the problems associated with traditional single-chamber reactor approaches. By separating the process of biological O_2 evolution and H_2 production, O_2-evolving autotrophs (such as cyanobacteria and green algae) can be used to facilitate H_2 production without the need to inhibit photosynthetic O_2 evolution directly. This approach negates the requirement for anoxygenic photosynthesis and thus cultures do not require regular cycles of oxygenic regeneration. As H_2 is produced in a separate chamber the product is relatively purer and more concentrated than in single-chamber designs. Furthermore, the process is not directly light-dependent, so H_2 can also be generated in the dark. BPE technology shows promise as a technique with exciting potential practical applications and appears to exhibit many unique and attractive attributes for renewable energy production.

Experimental

Cultures and growth

A wild-type strain of *Synechocystis* sp. PCC 6803 (referred to subsequently as *Synechocystis*) was from a laboratory stock.[24] A "triple-knockout" *Synechocystis* mutant from which all the three respiratory terminal oxidases (cytochrome bd oxidase [cyd], cytochrome c oxidase [cox] and alternative respiratory terminal oxidase [ARTO]) were absent was generated as described by Lea-Smith *et al.*[49] Cultures were grown and then analysed in BG11 medium[50] (low salt) or BG11 medium containing NaCl (0.25 M) (high salt). All cultures were supplemented with 5 mM $NaHCO_3$ and maintained at 22 ± 2 °C under low light (*ca.* 5 W m^{-2}) in a 24 h light cycle (12 h light/dark) under sterile conditions. Media conductivities were calculated using a Jenway conductivity meter 4310 (Jenway, Cambridge, UK) set at a reference temperature of 25 °C.

Strains were periodically streaked out and grown on agar plates containing agar (0.5–1.0%) and BG11, which were then used to inoculate fresh liquid cultures. Culture growth and density were monitored by spectrophotometric determination of chlorophyll content. Chlorophyll was extracted in 99.8% (v/v) methanol (Sigma-Aldrich, Gillingham, UK) as described previously.[51]

BPE construction and operation

The device consisted of a Perspex anodic chamber (300 ml) and cathodic chamber (50 ml) separated by a cation exchange Nafion® 115 perfluorinated membrane (Sigma-Aldrich, MO, USA) (1256 mm^2) (Fig. 1). Transparent indium tin oxide (ITO, 60 Ω sq^{-1}) coated onto polyethylene terephthalate (PET) (Sigma-Aldrich) was used as the anodic electrode (total area 3768 mm^2). The cathode consisted of a 1256 mm^2 platinised (1 μm thick) titanium electrode (Ti-Shop, London, UK).

During operation, the anodic chamber was inoculated with *Synechocystis* (10 nmol Chl ml^{-1}) containing $(Fe[CN]_6)^{3-}$ (1 mM) and the cathode chamber filled with the respective sterile media. The solutions in both chambers were continuously stirred with a magnetic stirring bar at 100 rpm. Under light conditions, an array of red LEDs (OVL-5528 [λ = 635 nm], Multicomp, UK) were positioned parallel to the anodic chamber resulted in an estimated photon flux density of 200 μE m^{-2} s^{-1} at the chamber surface using SKP 200 Light Meter (Skye Instruments Ltd, Llandrindod Wells, UK). Ambient temperatures within the device were monitored with a sensor probe (Uni-Trend Limited, Hong Kong, China) positioned inside the anodic chamber. All experiments were carried out at 22 ± 2 °C.

To initiate H_2 production, the cathodic chamber was sparged with nitrogen gas for 20 minutes and the light was turned off. A fixed bias-potential (1.0–1.4 V) was applied to the reactor circuit using a power box. A resistor (100 Ω) was connected in series with the power supply, and the voltage across the resistor was measured using an ADC-20 High Resolution Data Logger (HRDL) and PicoLog Data logging software version R5.21.5 (Pico Technology, St Neots, UK) to calculate the current.

Potassium ferricyanide measurements

At regular intervals, samples (1 ml) were taken from the anodic chamber, cells removed by rapid centrifugation, and the concentration of $(Fe[CN]_6)^{3-}$ in the supernatant measured spectrophotometrically at 420 nm (E_{420} = 1.02 mM^{-1} cm^{-1}) as described by Davey *et al.* (2003).

Hydrogen and oxygen production

Photosynthetic O_2 evolution rates were determined on concentrated cultures (~10 nmol Chl ml^{-1}) at 22 ± 2 °C with a

Dissolved Oxygen Meter (Extech Instruments Corporation, MA, USA) in media containing $(Fe[CN]_6)^{3-}$ (1 mM). Following dark equilibration (5–10 min), O_2 exchange rates were recorded for 5 min at increasing light intensities (0–280 μE m^{-2} s^{-1}) followed immediately by 5 min in darkness to calculate the average photosynthetic O_2 evolution and respiration rate, respectively. The respiration rate following illumination at each light intensity was subtracted to estimate the true rate of photosynthetic O_2 evolution (Fig. 2). Light response curves were analysed as described in Akhkha *et al.*[52] to determine the rate of maximum photosynthetic O_2 evolution (P_{max}) and apparent PSII quantum efficiency (AQE). Predicted values for actual quantum efficiency at P_{max} (QE_{max}) and the efficiency of $(Fe[CN]_6)^{3-}$ reduction at P_{max} ($FeCN^-{}_{QE}$) were derived for each culture as follows:

$$QE_{max} = \frac{P \times 4}{0.5 \times I}$$

$$FeCN^-{}_{QE} = \frac{F_r}{P \times 4}$$

where P is the photosynthetic O_2 evolution rate at P_{max} (μmol O_2 m^{-2} s^{-1}), I is the corresponding light intensity used and F_r is the rate of $(Fe[CN]_6)^{3-}$ reduction. In the cathode, O_2 evolution and uptake were measured using a Clark-type O_2 electrode. H_2 concentrations were measured using a Laboratory H_2 Microsensor (AMT Analysenmesstechnik GmbH, Germany). Coulombic efficiency (C_E) was calculated as the ratio of electrons recovered from $(Fe[CN]_6)^{4-}$ that were available for H_2 production at the cathode:

$$C_E = \frac{E}{F_o}$$

where E is the charge (μmol electrons per h) and F_o is the rate of $(Fe[CN]_6)^{4-}$ oxidation. Cathodic H_2 recovery (r_{cat}) and overall H_2 recovery (r_{H_2}) were calculated as described in Logan and Call.[17]

Statistical analysis

Results were subjected to analysis of variance (ANOVA) or Student's *t*-tests to determine the significance of the difference between responses to treatments. When ANOVA was performed.

Tukey's honestly significant difference (HSD) post-hoc tests were conducted to determine the differences between the individual treatments (SPSS Ver. 11.5; SPSS Inc., Chicago, IL, USA).

Acknowledgements

The authors are grateful for funding provided by the UK Engineering and Physical Sciences Research Council (EPSRC).

References

1 K. Christopher and R. Dimitrios, *Energy Environ. Sci.*, 2012, **5**, 6640–6651.
2 I. K. Kapdan and F. Kargi, *Enzyme Microb. Technol.*, 2006, **38**, 569–582.
3 H. S. Lee, W. F. Vermaas and B. E. Rittmann, *Trends Biotechnol.*, 2010, **28**, 262–271.
4 D. Dutta, D. De, S. Chaudhuri and S. K. Bhattacharya, *Microb. Cell Fact.*, 2005, **4**, 36.
5 A. Melis, *Planta*, 2007, **226**, 1075–1086.
6 E. Eroglu and A. Melis, *Bioresour. Technol.*, 2011, **102**, 8403–8413.
7 A. Melis, L. Zhang, M. Forestier, M. L. Ghirardi and M. Seibert, *Plant Physiol.*, 2000, **122**, 127–135.
8 A. S. Fedorov, S. Kosourov, M. L. Ghirardi and M. Seibert, *Appl. Biochem. Biotechnol.*, 2005, **121**, 403–412.
9 F. Gutthann, M. Egert, A. Marques and J. Appel, *Biochim. Biophys. Acta*, 2007, **1767**, 161–169.
10 T. Flynn, M. L. Ghirardi and M. Seibert, *Int. J. Hydrogen Energy*, 2002, **27**, 1421–1430.
11 L. Cournac, G. Guedeney, G. Peltier and P. M. Vignais, *J. Bacteriol.*, 2004, **186**, 1737–1746.
12 R. Surzycki, L. Cournac, G. Peltier and J.-D. Rochaix, *Proc. Natl. Acad. Sci. U. S. A.*, 2007, **104**, 17548–17553.
13 A. E. Marques, A. T. Barbosa, J. Jotta, M. C. Coelho, P. Tamagnini and L. Gouveia, *Biomass Bioenergy*, 2011, **35**, 4426–4434.
14 B. E. Logan, D. Call, S. Cheng, H. V. M. Hamelers, T. H. J. A. Sleutels, A. W. Jeremiasse and R. A. Rozendal, *Environ. Sci. Technol.*, 2008, **42**, 8630–8640.
15 H. Liu, S. Grot and B. E. Logan, *Environ. Sci. Technol.*, 2005, **39**, 4317–4320.
16 S. Cheng and B. E. Logan, *Proc. Natl. Acad. Sci. U. S. A.*, 2007, **104**, 18871–18873.
17 D. Call and B. E. Logan, *Environ. Sci. Technol.*, 2008, **42**, 3401–3406.
18 T. Yagishita, T. Horigome and K. Tanaka, *J. Chem. Technol. Biotechnol.*, 1993, **56**, 393–399.
19 M. Rosenbaum, U. Schröder and F. Scholz, *Appl. Microbiol. Biotechnol.*, 2005, **68**, 753–756.
20 J. M. Pisciotta, Y. Zou and I. V. Baskakov, *PLoS One*, 2010, **5**, e10821.
21 P. Bombelli, R. W. Bradley, A. M. Scott, A. J. Philips, A. J. McCormick, S. M. Cruz, A. Anderson, K. Yunus, D. S. Bendall, P. J. Cameron, J. M. Davies, A. G. Smith, C. J. Howe and A. C. Fisher, *Energy Environ. Sci.*, 2011, **4**, 4690–4698.
22 A. J. McCormick, P. Bombelli, A. M. Scott, A. J. Philips, A. G. Smith, A. C. Fisher and C. J. Howe, *Energy Environ. Sci.*, 2011, **4**, 4699–4709.
23 P. Bombelli, M. Zarrouati, R. J. Thorne, K. Schneider, S. J. L. Rowden, A. Ali, K. Yunus, P. J. Cameron, A. C. Fisher, D. I. Wilson, C. J. Howe and A. J. McCormick, *Phys. Chem. Chem. Phys.*, 2012, **14**, 12221–12229.
24 C. Herrero, A. Quaranta, W. Leibl, A. W. Rutherford and A. Aukauloo, *Energy Environ. Sci.*, 2011, **4**, 2353–2365.
25 D. Bora, A. Braun and E. C. Constable, *Energy Environ. Sci.*, 2013, **6**, 407–425.
26 B. Min, S. Cheng and B. E. Logan, *Water Res.*, 2005, **39**, 1675–1686.
27 J. A. Lynnes, T. L. M. Derzaph and H. G. Weger, *Planta*, 1998, **204**, 360–365.

28 N. A. Nimer, M. X. Ling, C. Brownlee and M. J. Merrett, *J. Phycol.*, 1999, **35**, 1200–1205.
29 M. S. Davey, D. J. Suggett, R. J. Geider and A. R. Taylor, *J. Phycol.*, 2003, **39**, 1132–1144.
30 A. M. Scott, M. Sc. Thesis, University of Cambridge, 2010.
31 G. Grigorieva and S. Shestakov, *FEMS Microbiol. Lett.*, 1982, **13**, 367–370.
32 T. Kaneko, S. Sato, H. Kotani, A. Tanaka, E. Asamizu, Y. Nakamura, N. Miyajima, M. Hirosawa, M. Sugiura, S. Sasamoto, T. Kimura, T. Hosouchi, A. Matsuno, A. Muraki, N. Nakazaki, K. Naruo, S. Okumura, S. Shimpo, C. Takeuchi, T. Wada, A. Watanabe, M. Yamada, M. Yasuda and S. Tabata, *DNA Res.*, 1996, **3**, 109–136.
33 D. L. Richardson, R. H. Reed and W. D. P. Stewart, *FEMS Microbiol. Lett.*, 1983, **18**, 99–102.
34 S. E. Hart, B. G. Schlarb-Ridley, D. S. Bendall and C. J. Howe, *Biochem. Soc. Trans.*, 2005, **33**, 832–835.
35 B. E. Logan, *Nat. Rev. Microbiol.*, 2009, **7**, 375–381.
36 D. R. Lovley, *Energy Environ. Sci.*, 2011, **4**, 4896–4906.
37 B. Yazici, *Turk. J. Chem.*, 1999, **23**, 301–308.
38 R. S. Berk and J. H. Canfield, *Appl. Microbiol.*, 1964, **12**, 10–12.
39 M. Mehanna, T. Saito, J. Yan, M. Hickner, X. Cao, X. Huang and B. E. Logan, *Energy Environ. Sci.*, 2010, **3**, 1114–1120.
40 Y. Kim and B. E. Logan, *Proc. Natl. Acad. Sci. U. S. A.*, 2011, **108**, 16176–16181.
41 H. Luo, P. Jenkins and Z. Ren, *Environ. Sci. Technol.*, 2011, **45**, 340–344.
42 A. Bandyopadhyay, J. Stöckel, H. Min, L. A. Sherman and H. B. Pakrasi, *Nat. Commun.*, 2010, **1**, 139.
43 S. Fulda, S. Mikkat, F. Huang, J. Huckauf, K. Martin, B. Norling and M. Hagemann, *Proteomics*, 2006, **6**, 2733–2745.
44 M. Hagemann, *FEMS Microbiol. Rev.*, 2011, **35**, 87–123.
45 S. Izawa, *Methods Enzymol.*, 1980, **69**, 413–434.
46 S. Kumar and S. K. Acharya, *Anal. Biochem.*, 1999, **268**, 89–93.
47 S. Cheng and B. E. Logan, *Bioresour. Technol.*, 2011, **102**, 3571–3574.
48 J.-Y. Nam, J. C. Tokash and B. E. Logan, *Int. J. Hydrogen Energy*, 2011, **36**, 10550–10556.
49 D. J. Lea-Smith, N. Ross, M. Zori, D. S. Bendall, J. S. Dennis, S. A. Scott, A. G. Smith and C. J. Howe, *Plant Physiol.*, 2013, **162**, 484–495.
50 R. Rippka, J. Deruelles, J. B. Waterbury, M. Herdman and R. Stanier, *J. Gen. Microbiol.*, 1979, **111**, 1–61.
51 R. J. Porra, W. A. Thompson and P. E. Kriedemann, *Biochim. Biophys. Acta*, 1989, **975**, 384–394.
52 A. Akhkha, I. Reid, D. D. Clarke and P. Dominy, *Planta*, 2001, **214**, 135–141.

